Dalton Transactions

PAPER

View Article Online
View Journal | View Issue

Cite this: *Dalton Trans.*, 2015, **44**, 18101

Rare-earth metal methylidene complexes with $Ln_3(\mu_3\text{-}CH_2)(\mu_3\text{-}Me)(\mu_2\text{-}Me)_3$ core structure†

Dorothea Schädle,[a] Melanie Meermann-Zimmermann,[b] Cäcilia Maichle-Mössmer,[a] Christoph Schädle,[a] Karl W. Törnroos[c] and Reiner Anwander*[a]

Received 30th July 2015,
Accepted 14th September 2015

DOI: 10.1039/c5dt02936h

www.rsc.org/dalton

Trinuclear rare-earth metal methylidene complexes with a $Ln_3(\mu_3\text{-}CH_2)(\mu_3\text{-}Me)(\mu_2\text{-}Me)_3$ structural motif were synthesized by applying three protocols. Polymeric $[LuMe_3]_n$ (**1**-Lu) reacts with the sterically demanding amine $H[NSiMe_3(Ar)]$ (Ar = $C_6H_3iPr_2$-2,6) in tetrahydrofuran *via* methane elimination to afford isolable monomeric $[NSiMe_3(Ar)]LuMe_2(thf)_2$ (**4**-Lu). The formation of trinuclear rare-earth metal tetramethyl methylidene complexes $[NSiMe_3(Ar)]_3Ln_3(\mu_3\text{-}CH_2)(\mu_3\text{-}Me)(\mu_2\text{-}Me)_3(thf)_3$ (**7**-Ln; Ln = Y, Ho, Lu) *via* reaction of $[LnMe_3]_n$ (**1**-Ln; Ln = Y, Ho, Lu) with $H[NSiMe_3(Ar)]$ is proposed to occur *via* an "intermediate" species of the type $[NSiMe_3(Ar)]LnMe_2(thf)_x$ and subsequent C–H bond activation. Applying Lappert's concept of Lewis base-induced methylaluminate cleavage, compounds $[NSiMe_3(Ar)]Ln(AlMe_4)_2$ (**5**-Ln; Ln = Y, La, Nd, Ho) were converted into methylidene complexes **7**-Ln (Ln = Y, Nd, Ho) in the presence of tetrahydrofuran. Similarly, tetramethylgallate complex $[NSiMe_3(Ar)]Y(GaMe_4)_2$ (**6**-Y) could be employed as a synthesis precursor for **7**-Y. The molecular composition of complexes **4**-Ln, **5**-Ln, **6**-Y and **7**-Ln was confirmed by elemental analyses, FTIR spectroscopy, ^1H and ^{13}C NMR spectroscopy (except for holmium derivatives) and single-crystal X-ray diffraction. The Tebbe-like reactivity of methylidene complex **7**-Nd with 9-fluorenone was assessed affording oxo complex $[NSiMe_3(Ar)]_3Nd_3(\mu_3\text{-}O)(\mu_2\text{-}Me)_4(thf)_3$ (**8**-Nd). The synthesis of **5**-Ln yielded $[NSiMe_3(Ar)]_2Ln(AlMe_4)$ (**9**-Ln; Ln = La, Nd) as minor side-products, which could be obtained in moderate yields when homoleptic $Ln(AlMe_4)_3$ were treated with two equivalents of $K[NSiMe_3(Ar)]$.

Introduction

Multiple metal–carbon bonds, predominantly alkylidene units "$M{=}CR_2$", continue to trigger immense research activities in organometallic synthesis and catalysis.[1–8] Schrock's neopentylidene complex $(tBuCH_2)_3Ta(=CHtBu)$[9,10] marked the first example of a stable transition metal alkylidene complex, with the bulky *t*Bu substituents at the α-carbon atom impeding intermolecular decomposition pathways. In contrast, methylidene "CH_2^{2-}" species are sterically less protected against bimolecular reactions, and hence present a particular challenge and are found to be kinetically labile. Although authenticated by single-crystal X-ray diffraction, the first transition metal methylidene complex $Cp_2Ta(CH_2)(CH_3)$ decomposes bimolecularly forming ethylene complex $Cp_2Ta(C_2H_4)(CH_3)$.[11,12] Current progress in the field of early transition metal terminal methylidene complexes features Mindiola's group 4 and group 5 derivatives $(PNP)M{=}CH_2(OAr)$ (M = Zr, Hf, PNP = $N[2\text{-}P(iPr)_2\text{-}4\text{-}CH_3\text{-}C_6H_3]_2$, Ar = $C_6H_3iPr_2$-2,6) and $(ArO)_2Nb{=}CH_2(H_2CPPh_3)$ (Ar = $C_6H_2(CHPh_2)_2$-2,6-*t*Bu-4).[13,14] Alternatively, stabilization of the methylidene moiety is achieved by delocalizing the negative charge over multinuclear, homometallic or heterobimetallic Lewis-acid stabilized complexes.[15–18] The most prominent example of a Lewis-acid stabilized heterobimetallic methylidene complex is the Tebbe reagent $Cp_2Ti[(\mu_2\text{-}CH_2)(\mu_2\text{-}Cl)AlMe_2]$,[5,19] whose structural elucidation proved to be delicate.[20] The Tebbe reagent also laid the ground work for a series of rare-earth metal variants, (L)Ln(III)-$(CH_2)_x(AlMe_2R)_y$ (L = monoanionic,[21–25] neutral ligand;[26–29] R = Me, ferrocenyl). Previous studies from our laboratory and others on rare-earth-metal(III) alkyl complexes (L)LnRR′ (L = C_5Me_5(= Cp*), $NSiMe_3(Ar)$, $PhC(NC_6H_3iPr_2\text{-}2,6)_2$; Ln = Y, La, Ho, Lu; R, R′ = Me, $AlMe_4$, Cl) led to the isolation of "Lewis-acid-free" Ln^{III} methylidene complexes with a striking $Ln_3(\mu_3\text{-}CH_2)$ core structure (Scheme 1).[30–32]

Experimental and theoretical studies on homometallic trinuclear rare-earth metal methylidene complexes $L_3Ln_3(\mu_3\text{-}CH_2)(\mu_3\text{-}CH_3)(\mu_2\text{-}CH_3)_3(thf)_n$ (L = monoanionic ligand) revealed Tebbe-like reactivity in methylenation reactions (Scheme 1)

[a]*Institut für Anorganische Chemie, Universität Tübingen, Auf der Morgenstelle 18, D-72076 Tübingen, Germany. E-mail: reiner.anwander@uni-tuebingen.de*
[b]*Dezernat Forschung, Technische Universität Darmstadt, Karolinenplatz 5, D-64289 Darmstadt, Germany*
[c]*Department of Chemistry, University of Bergen, Allégaten 41, N-5007 Bergen, Norway*

†Electronic supplementary information (ESI) available: Spectroscopic and crystallographic data. CCDC 1410385–1410394. For ESI and crystallographic data in CIF or other electronic format see DOI: 10.1039/c5dt02936h

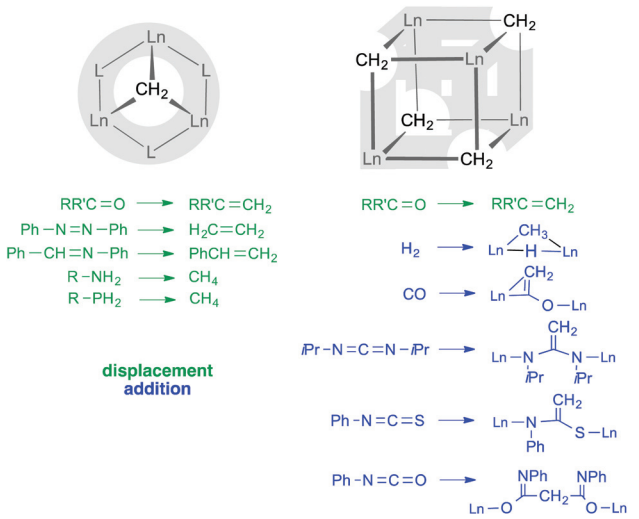

Scheme 1 Stabilization and reactivity of CH_2^{2-} methylidene moieties in trigonal pyramidal and cuboid arrangements with Ln(III) centres.

along with methylation of the carbonylic functionalities.[31–33] In sharp contrast, treatment of $Cp'_3Tm_3(\mu_3\text{-}CH_2)(\mu_3\text{-}CH_3)(\mu_2\text{-}CH_3)_3$ (Cp' = $C_5Me_4SiMe_3$) with a ketone would rather yield $Cp'_3Tm_3(\mu_2\text{-}CH_3)_3[OC(CH_3)(C_6H_4)_2)]$ as a result of methylidene transfer and simultaneous *ortho*-metallation of benzophenone (not shown in Scheme 1).[34] Moreover, Hou and coworkers accessed "Lewis-acid-free" cuboid clusters $[Cp'Ln(\mu_3\text{-}CH_2)]_4$ *via* prolonged thermal treatment of the respective trinuclear complexes $Cp'_3Tm_3(\mu_3\text{-}CH_2)(\mu_3\text{-}CH_3)(\mu_2\text{-}CH_3)_3$ or $Cp'_3Lu_3(\mu_2\text{-}CH_3)_6$, respectively. While such Lewis-acid-free Ln(III)–CH_2^{2-} clusters revealed interesting reactivity toward (electronically unsaturated) functional substrates (Scheme 1),[35–37] seemingly less efforts were devoted to elucidate the formation of such rare-earth metal methylidene species. Herein, we present three synthesis approaches toward rare-earth metal tetramethyl methylidene complexes capable of methylenating ketones. The isolation of dimethyl complex $[NSiMe_3(Ar)]LuMe_2(thf)_2$ hints to a mechanism with one crucial C–H bond activation step. Part of the work on methylidene complexes $[NSiMe_3(Ar)]_3Ln_3(\mu_3\text{-}CH_2)(\mu_3\text{-}CH_3)(\mu_2\text{-}CH_3)_3(thf)_3$ (7-Ln, Ln = Y, Ho, Lu) were recently communicated by our group.[31]

Results and discussion

We have shown previously that treatment of $[LnMe_3]_n$ (**1**-Ln; Ln = Y, Ho, and Lu)[31,38] suspended in *n*-hexane with one equivalent of $H[NSiMe_3(Ar)]$ and subsequent addition of excess thf at ambient temperature, selectively yields the trinuclear rare-earth metal complexes $[NSiMe_3(Ar)]_3Ln_3(\mu_3\text{-}CH_2)(\mu_3\text{-}CH_3)(\mu_2\text{-}CH_3)_3(thf)_3$ (7-Ln, Ln = Y, Ho, Lu; Scheme 2, route **A**).[31] Due to the insolubility of **1**-Ln in aliphatic solvents, immediate reaction with $H[NSiMe_3(Ar)]$ in *n*-hexane to form putative $[NSiMe_3(Ar)]LnMe_2$ did not occur. It is anticipated that the donor solvent (thf) is necessary to break up the polymeric network of **1**-Ln, thus initiating the reaction. Re-investigation of the lutetium-reaction afforded single crystals of $[NSiMe_3(Ar)]LuMe_2(thf)_2$ (**4**-Lu, 33%), which could be isolated together with precipitated $[NSiMe_3(Ar)]_3Lu_3(\mu_3\text{-}CH_2)(\mu_3\text{-}Me)(\mu_2\text{-}Me)_3(thf)_3$ (7-Lu, 19%). The ^{1}H NMR spectrum of **4**-Lu in thf-d_8 at ambient temperature features one set of signals for the amido ligand and the coordinated thf donor molecules. The Lu–CH_3 moieties appeared as one narrow singlet at −1.06 ppm (6H), indicating a highly fluxional nature of complex **4**-Lu. Cooling a solution of **4**-Lu in thf-d_8 to −90 °C significantly shifted the resonances of the metal-bonded methyl groups, the silyl moiety and the methine groups (iPr) to lower field, while the signals for the aryl hydrogen atoms and the methyl groups appeared at higher fields (Fig. S9†). The high thermal sensitivity of compound **4**-Lu allowed $^{13}C\{^1H\}$ NMR spectroscopy only at low temperatures (−35 °C) revealing the signal for the Lu–CH_3 groups at 29.5 ppm.

Single-crystal X-ray diffraction of **4**-Lu revealed a geometry about the five-coordinate lutetium metal centre which can best be described as distorted trigonal bipyramidal with C1, C2, and N1 occupying the positions in the equatorial plane and O1 and O2 in the apical positions (see Fig. 1). The Lu–C(CH_3) bond lengths of 2.366(4) and 2.378(5) Å of complex **4**-Lu are in the same range as in dimethyl complex $(Tp^{tBu,Me})LuMe_2$ (avg. 2.370 Å)[39] and ate complex $[NSiMe_3(Ar)]_2YbMe(\mu\text{-}Me)Li(thf)_3$ (Ar = $C_6H_3iPr_2$-2,6; Ln–C 2.349(8) Å, 2.382(7) Å; Ln–N avg. 2.226 Å),[40] but the Ln–C/N bond lengths of **4**-Lu are slightly longer than in 4-coordinate $[NSiMe_3(Ar)]Lu(CH_2SiMe_3)_2(thf)$ (Ar = $C_6H_3iPr_2$-2,6; Lu–C avg. 2.318 Å; Ln–N 2.153(2) Å).[41] The sterically demanding amido ligand seems suitable for protecting the methyl groups kinetically. However, decomposition of compound **4**-Lu starts at ambient temperature within just a few hours, which is consistent with the hypothesis that **4**-Lu is a crucial intermediate in the synthesis of 7-Lu. Although the exact mechanism for the formation of multinuclear methylidene complexes is unclear, we assume that species like $[NSiMe_3(Ar)]LnMe_2(thf)_x$ play a pivotal role.

The isolation of dimethyl complex $[NSiMe_3(Ar)]LuMe_2(thf)_2$ (**4**-Lu) as a plausible intermediate in the formation of the trinuclear complex 7-Lu tempted us to speculate about a possible mechanism (see Scheme 3). The reaction proceeds presumably *via* a sequence of methane elimination (**a**) or donor-induced tetramethylaluminate/gallate cleavage (*vide infra*) (**b**) to yield dimethyl complexes (**I**^{1} or **4**-Lu), C–H bond activation under formation of Ln(III)=CH_2 (**I**^{2}) and methane (**c**) and subsequent agglomeration (**d**) affording trinuclear compounds 7-Ln, which consist of a core with three rare-earth metal centres bridged by μ_2-Me, μ_3-Me and μ_3-CH_2 moieties.

The formation of 7-Y by donor-induced cleavage of bis(aluminate) complex **5**-Y (Scheme 2, route **B**; Scheme 3, **b**–**d**) was also previously communicated by us.[31] We now found that route **B** can be adopted for the larger rare-earth metal centres, which is infeasible for route **A**. Reaction of homoleptic $Ln(AlMe_4)_3$ (**3**-Ln, Ln = Y, La, Nd, Ho)[42,43] with one equivalent of potassium amide $K[NSiMe_3(Ar)]$[44,45] in *n*-hexane at ambient temperature cleanly formed the respective rare-earth metal

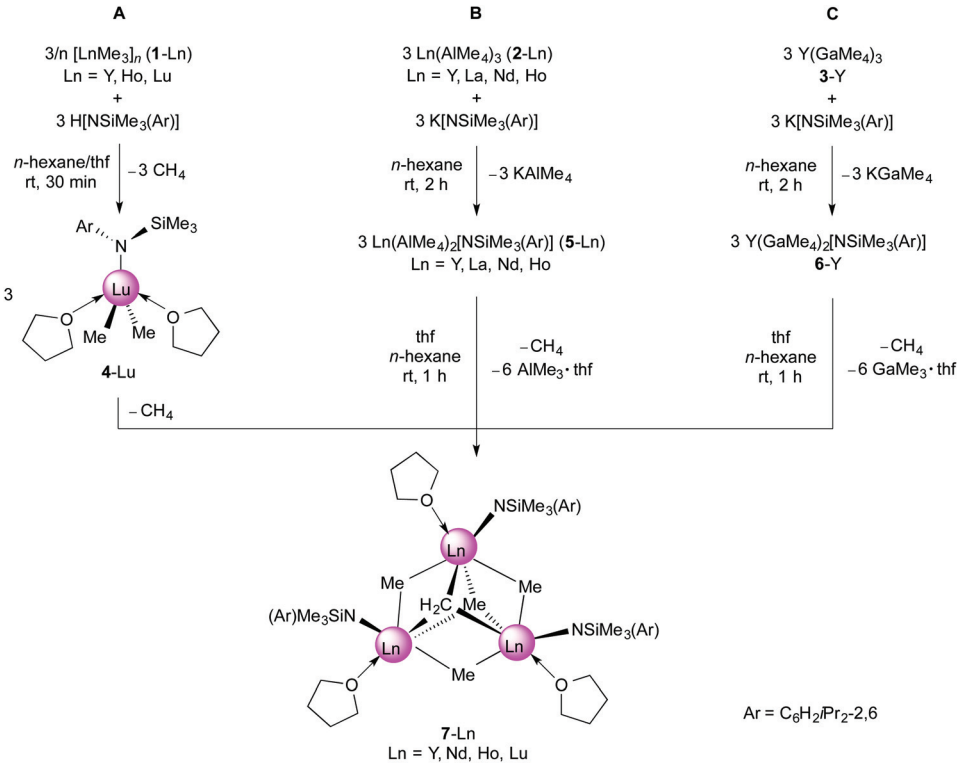

Scheme 2 Syntheses of trinuclear rare-earth metal methylidene complexes **7**-Ln supported by a bulky amido ligand.

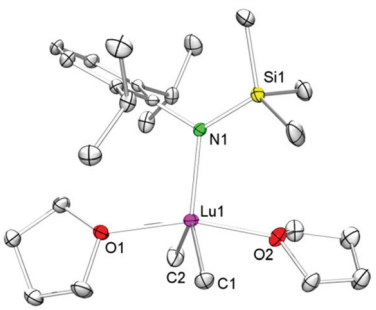

Fig. 1 Molecular structure of **4**-Lu (atomic displacement parameters are set at the 30% level). Hydrogen atoms are omitted for clarity. Selected bond lengths [Å] and angles [°]: Lu1–C1 2.366(4), Lu1–C2 2.378 (5), Lu1–O1 2.312(3), Lu1–O2 2.333(3), Lu1–N1 2.203(3), C6–N1–Lu1 112.8(2), O1–Lu1–O2 161.6(1), O1–Lu1–C1 88.1(1), O2–Lu1–C1 86.6(1), O1–Lu1–C2 83.1(1), O2–Lu1–C2 84.8(1), C1–Lu1–C2 122.3(2).

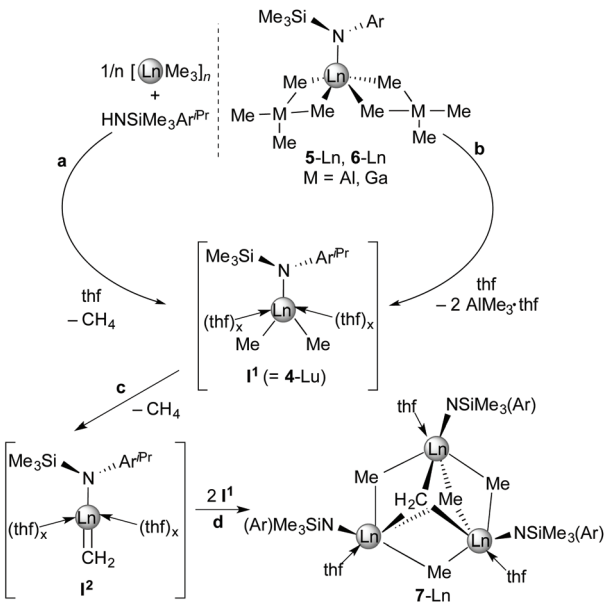

Scheme 3 Proposed reaction mechanism for the formation of multinuclear methylidene complexes **7**-Ln.

mono(amide) complexes $[NSiMe_3(Ar)]Ln(AlMe_4)_2$ (**5**-Ln) in high yields (Scheme 2). The molecular composition of complexes **5**-Ln was confirmed by elemental analyses, infrared spectroscopy, single-crystal X-ray diffraction and $^1H/^{13}C$ NMR spectroscopy (except **5**-Ho).

The ^1H NMR spectra of the diamagnetic complexes **5**-Ln (Ln = Y, La) showed the expected resonances for the $NSiMe_3(Ar)$ ligand. The methyl groups of the $Al(\mu\text{-}Me)_2Me_2$ moieties appeared as one narrow signal indicating a rapid exchange of bridging and terminal methyl groups (**5**-Y δ –0.24 ppm, $^2J_{YH}$ = 2.5 Hz; **5**-La δ –0.19 ppm). Good quality ^1H and ^{13}C NMR spectra could also be obtained for the paramagnetic neodymium compound **5**-Nd. However, due to significant paramagnetic shifts and broadening effects, assignment of the

signals – except for the $AlMe_4$ resonance at 11.27 ppm in the ^1H NMR spectrum – appeared to be difficult.

The X-ray crystallographic analyses of $[NSiMe_3(Ar)]Ln(AlMe_4)_2$ (**5**-Ln) revealed structural motifs as found in the solid-state structures of half-sandwich bis(tetramethylaluminate) complexes $Cp^RLn(AlMe_4)_2$ [46–48] with one $AlMe_4$ ligand coordinating in the routinely observed planar η^2 fashion, and the second one showing a bent η^2 coordination (Fig. 2 and S1–S3†). The geometry about the five-coordinate Ln(III) centre can best be described as distorted square pyramidal, with the four bridging methyl groups in the corner of the basal plane and the amido nitrogen atom in the apical position. As detected for $Cp^RLn(AlMe_4)_2$ [46–48] the Ln–C(μ-Me) bond lengths increase with increasing Ln(III) size, the bonds in the bent $AlMe_4$ ligand being significantly elongated compared to those in the planar tetramethylaluminate ligand, and C8 is tilted toward the rare-earth metal centre. The solid-state structures of **5**-Ln feature additional short contacts between the metal centres and the *ipso* carbon atoms of the aryl rings. As a consequence, the aryl ring lies almost orthogonally to the Ln–N bond as evidenced by the acute C9–N1–Ln1 bond angles (Table 1). Interestingly, the feasibility of complexes **5**-La and **5**-Nd might provide access to methylidene complexes of type **7**-Ln with large rare-earth metal centres.

The anticipated formation of a transient $[NSiMe_3(Ar)]LnMe_2(thf)_x$ species is substantiated by synthesis approach **B** (Scheme 2), since addition of excess thf to *n*-hexane solutions of $[NSiMe_3(Ar)]Ln(AlMe_4)_2$ (**5**-Ln) afforded complexes **7**-Ln in high yields. Single-crystal X-ray diffraction revealed the formation of trinuclear rare-earth metal tetramethyl methylidene complexes $[NSiMe_3(Ar)]_3Ln_3(\mu_3\text{-}CH_2)(\mu_3\text{-}Me)(\mu_2\text{-}Me)_3(thf)_3$ (**7**-Ln, Ln = Y,[31] Nd, Ho) as the product of sequential donor-induced cleavage of $Ln(\mu_2\text{-}Me)_2(AlMe_2)$ moieties,[49] C–H bond activation, and agglomeration (Schemes 2 and 3). Note that, treatment of **5**-La with excess thf led to intractable, alkylated species.[24] Comparative studies on half-sandwich dialkyl complexes revealed that the capability of alkyl complexes to engage in C–H bond activation reactions strongly depends on the size of the rare-earth metal centre, the amount of Lewis base as well as the steric demand of the ancillary ligand. For example, Hou and coworkers showed that the reaction of $Cp'Ln(CH_2SiMe_3)_2(thf)$ ($Cp' = C_5Me_4SiMe_3$) with $AlMe_3$ in diethyl ether at ambient temperature yielded $[Cp'LnMe_2]_3$ for lutetium and $Cp'_3Ln_3(\mu_3\text{-}CH_2)(\mu_3\text{-}Me)(\mu_2\text{-}Me)_3$ for thulium.[34] We found that the donor-induced cleavage of $Cp^*Ln(AlMe_4)_2$ (Ln = Y, Lu) with two equivalents of tetrahydrofuran led to trimeric $[Cp^*LnMe_2]_3$, whereas the reaction with one equivalent thf produced methylidyne complex $[Cp^*_4Y_4(\mu_2\text{-}CH_3)_2\{(CH_3)Al(\mu_2\text{-}CH_3)_2\}_4(\mu_4\text{-}CH)_2]$.[47,50]

Table 1 Selected structural parameters [Å, °] of complexes **5**-La, **5**-Nd, **5**-Ho and **6**-Y[a]

	5-La	**5**-Nd[a]	**5**-Ho[a]	**6**-Y
Ln–N1	2.295(4)	2.222(2)	2.160(3)	2.172(4)
Ln–C1	2.712(5)	2.617(3)	2.524(4)	2.522(5)
Ln–C2	2.716(5)	2.661(4)	2.525(4)	2.520(5)
Ln–C5	2.837(5)	2.661(4)	2.631(4)	2.653(5)
Ln–C6	2.717(5)	2.718(3)	2.585(4)	2.585(5)
Ln···M1	3.278(2)	3.194(1)	3.078(1)	3.0550(7)
Ln···M2	3.013(1)	2.976(1)	2.882(1)	2.8711(7)
Ln···C9	2.779(4)	2.755(3)	2.694(3)	2.770(4)
Ln–N1–C9	93.8(2)	95.7(2)	95.4(2)	98.5(2)
Ln–C1–M1–C2	−0.4(2)	9.6(2)	7.7(2)	42.1(2)
Ln–C5–M2–C6	45.5(2)	−40.0(1)	−40.4(2)	9.5(2)

[a] Metric parameters of molecule 2 of **5**-Nd and **5**-Ho are listed in the ESI.

Organoaluminum moieties are well-known to promote C–H bond activation reactions at transition metals.[19,50–52] As such, we were interested to elucidate the influence of any coordinated alkylaluminate moieties on the formation of **7**-Ln along pathway **B**. According to Pearson's HSAB concept the methyl groups in $GaMe_4$ moieties should behave less basic than in $AlMe_4$. This is also in accord with the tendency of the tetramethylgallato ligand to separate off $GaMe_3$. Hence we tackled the synthesis of $[NSiMe_3(Ar)]Y(GaMe_4)_2$ (**6**-Y) from homoleptic $Y(GaMe_4)_3$ (**2**-Y)[53,54] which was obtained aluminium-free from $[Y(NMe_2)_3(LiCl)_3]$ and $GaMe_3$. Reaction of **2**-Y with one equivalent of potassium amide $K[NSiMe_3(Ar)]$[44,45] in *n*-hexane at ambient temperature gave exclusively compound **6**-Y in high yields (Scheme 2, route **C**). Comparable to aluminate complexes **5**-Ln, **6**-Y features a highly fluxional Ga $(\mu\text{-}Me)_2Me_2$ coordination as evidenced by one narrow signal for the methyl groups at δ −0.03 ppm. The ^{89}Y NMR resonance of **6**-Y (δ 477.2 ppm) is in the same range as for **7**-Y (δ 498.0 ppm).[31] The molecular structure of complex **6**-Y is isomorphous to those of **5**-Ln and similar to $Cp^*Y(GaMe_4)_2$ ($Cp^* = C_5Me_5$) regarding the coordination of the $GaMe_4$ ligands (Fig. 3).[55]

The metrical parameters of **6**-Y are comparable to $Cp^*Y(GaMe_4)_2$ with average Y–C(μ-CH_3) bond lengths of 2.616 Å and 2.520 Å for the bent and planar $Ga(\mu\text{-}Me)_2Me_2$ moieties, respectively, being slightly shorter than in the respective half-

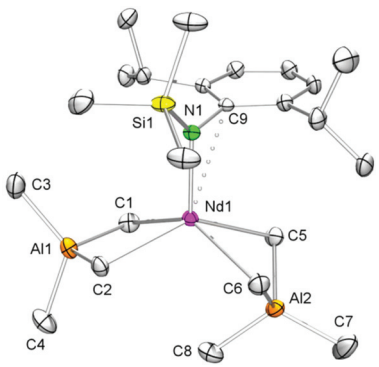

Fig. 2 Molecular structure of $[NSiMe_3(Ar)]Nd(AlMe_4)_2$ (**5**-Nd), representative of the isostructural complexes **5**-La, **5**-Nd and **5**-Ho. Atomic displacement parameters are set at the 30% level, hydrogen atoms have been omitted for clarity. The asymmetric unit contains two independent molecules with similar structural data.

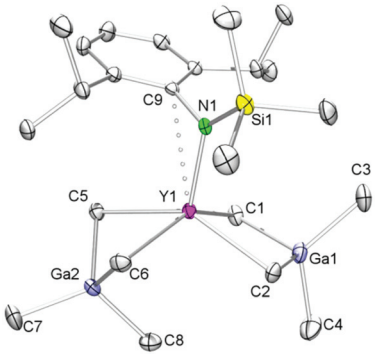

Fig. 3 Molecular structure of $[NSiMe_3(Ar)]Y(GaMe_4)_2$ (**6**-Y). Atomic displacement parameters are set at the 30% level, hydrogen atoms have been omitted for clarity.

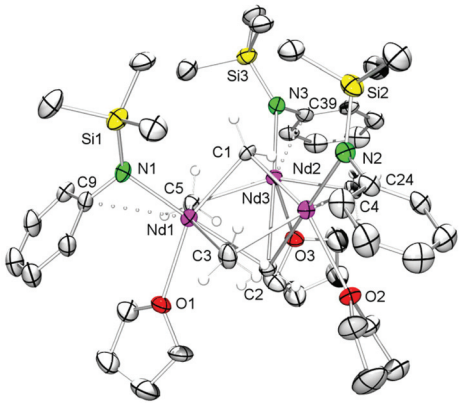

Fig. 4 Molecular structure of **7**-Nd (atomic displacement parameters are set at the 30% level). Solvent molecules, isopropyl groups and hydrogen atoms, except for Nd–CH_2 and Nd–CH_3 moieties, have been omitted for clarity.

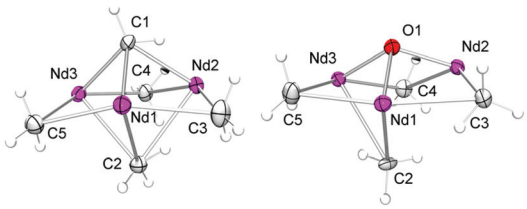

Fig. 5 Molecular core structure of **7**-Nd (left) and **8**-Nd (right). Atomic displacement parameters are set at the 30% level.

sandwich complex (average 2.679 and 2.555 Å).[55] The Ln–C bond lengths of the related yttrium neosilyl complexes $[NSiMe_3(Ar)]Y(CH_2SiMe_3)_2(thf)$ (Ar = $C_6H_3iPr_2$-2,6; Y–C avg. 2.367 Å)[41] and $[NSiiPr_3(Ar)]Y(CH_2SiMe_3)_3Li(thf)_2$ (Ar = $C_6H_3iPr_2$-2,6; Y–C 2.373(3)–2.490(4) Å)[56] are as expected shorter than in **6**-Y, but the Ln–N(amido) bond lengths compare well (2.190(2) Å;[41] 2.259(3) Å;[56] **6**-Y, 2.172(4) Å).

If the organoaluminum moieties in $[NSiMe_3(Ar)]Ln(AlMe_4)_2$ (**5**-Ln) would be crucial for the formation of methylidene species, the reaction of the respective methylgallate $[NSiMe_3(Ar)]Y(GaMe_4)_2$ (**6**-Y) with a Lewis base might yield a species like $\{[NSiMe_3(Ar)]YMe_2\}_x$. However, upon treatment of **6**-Y with thf we could isolate $[NSiMe_3(Ar)]_3Y_3(\mu_3\text{-}CH_2)(\mu_3\text{-}Me)(\mu_2\text{-}Me)_3(thf)_3$ (**7**-Y) in almost quantitative yield.

The rare-earth metal tetramethyl methylidene complexes **7**-Ln are sparingly soluble in *n*-hexane, but readily dissolve in aromatic solvents and thf, which allowed for elaborate NMR spectroscopic investigations of the diamagnetic representatives **7**-Y and **7**-Lu.[31] The interpretation of the ^1H NMR spectra of compounds **7**-Ln (Ln = Nd, Ho) is affected by paramagnetic shifts and line broadening.

Representatively for the isostructural complexes **7**-Ln, Fig. 4 and 5 illustrate the molecular and core structure of the neodymium derivative **7**-Nd (**7**-Ho: Fig. S5†). Complexes **7**-Nd and **7**-Ho are isomorphous to the previously reported **7**-Y and **7**-Lu,[31] crystallizing in the monoclinic space group $P2_1\bar{n}$. In the solid state, each Ln is six-coordinate by one amido ligand, one thf, three bridging methyl groups, and one μ_3-bridging methylidene group. The core atoms of the complex (Fig. 5, left) adopt a distorted hexagonal bipyramid with alternating Ln and μ_2-bridging methyl groups in the equatorial, and the μ_3-methyl and the methylidene groups in the apical positions. Together with the methylidene group all three amido ligands are residing on one side of the plane spanned by the Ln metal centres. It seems that the amido substituents provide a protective enclosure for the methylidene moiety reminiscent of a picket fence, thus impeding intermolecular deactivation.[57] The $Ln_3(\mu_3\text{-}CH_2)$ unit in **7**-Ln resembles those previously found in complexes $L_3Ln_3(\mu_3\text{-}CH_2)(\mu_3\text{-}Me)(\mu_2\text{-}Me)_3(thf)_x$ (Ln = Sc, Y, Ho, Tm, Lu; x = 0, 1).[31,32,34] The Ln–C(CH_2) bond lengths of 2.356(10)–2.428(10) Å in **7**-Ho (**7**-Nd: 2.425(7)–2.505(8) Å) are in accord with the distances reported for **7**-Y (2.345(5)–2.424(4) Å),[31] but are significantly shorter than the values for $Cp^*_3Ln_3(\mu_3\text{-}CH_2)(\mu_3\text{-}Cl)(\mu_2\text{-}Cl)_3$ (Y: 2.424(2)–2.450(2) Å, La: 2.537(3)–2.635(3) Å)[30] considering the differences of the ionic radii. As expected, the Ln–C bond lengths of the μ_2-CH_3 moieties are between the values for Ln–C(μ_3-CH_2) and Ln–C(μ_3-CH_3) (Table 2).

Reaction of 7-Ln with ketones

In the presence of carbonylic substrates, methylidene complexes **7**-Ln act as Schrock-type nucleophilic carbenes. Moni-

Table 2 Selected average bond lengths (Å) and angles (°) for **7**-Nd, **7**-Ho and **8**-Nd

	7-Nd	7-Ho	8-Nd
Ln–C(μ_3-CH_2)	2.475	2.391	
Ln–C(μ_3-CH_3)	2.817	2.737	
Ln–C(μ_2-CH_3)	2.635	2.547	2.676
Ln–O(oxo)			2.239
Ln–N	2.355	2.279	2.369
Ln–O(thf)	2.568	2.466	2.543
Ln–C_{ipso}(Ar)	3.021	3.086	3.076

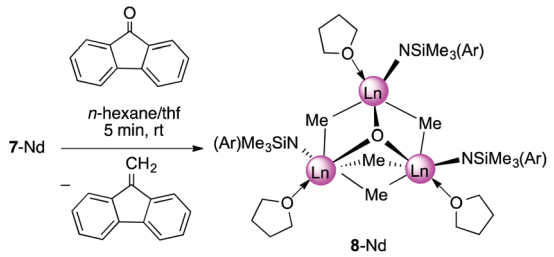

Scheme 4 Synthesis of $[NSiMe_3(Ar)]_3Nd_3(\mu_3\text{-}O)(\mu_2\text{-}Me)_4(thf)_3$ (**8**-Nd).

toring the reactions of 7-Ln with 1 equivalent of 9-fluorenone, benzophenone, and cyclohexanone, respectively, by ^{1}H NMR spectroscopy, clearly revealed the formation of the expected methylenated products (see Scheme 4) and concomitantly led to methylation products.[31] If compared to the original Tebbe reagent, which allows a variety of functional substrates (esters, lactones) suppressing the formation of undesired side-products,[58] complexes of type 7-Ln are certainly less efficient and selective.[30] Theoretical studies on $[PhC(NC_6H_3iPr_2\text{-}2,6)_2]_3Sc_3(\mu_3\text{-}CH_2)(\mu_3\text{-}Me)(\mu_2\text{-}Me)_3$, however, indicated that methylidene transfer rather than methyl transfer occurs.[33]

Upscaling of the reaction between 7-Nd and 9-fluorenone (1 : 1 ratio) in *n*-hexane/thf led to the formation of 9-methylidene-fluorene and $[NSiMe_3(Ar)]_3Nd_3(\mu_3\text{-}O)(\mu_2\text{-}Me)_4(thf)_3$ (**8**-Nd) as indicated by an immediate colour change from blue to green (Fig. S21†). NMR-scale reactions using 1–5 equivalents of the carbonylic reagent in benzene-d_6, revealed that after addition of the third equivalent of substrate the mixture kept a brown colour. Additional signals assignable to a paramagnetically shifted 9-methyl-9*H*-fluoren-9-yloxy moiety were observed as well, however, due to the existing paramagnetism, a quantification of methylenation *versus* methylation was infeasible. Single-crystal X-ray diffraction of complex **8**-Nd revealed that the core structure of 7-Nd (Fig. 5, left) was replaced by $Nd_3(\mu_3\text{-}O)(\mu_2\text{-}Me)_4$ with the Nd^{III} metal centres being bridged by one μ_3-oxo moiety and four μ_2-Me groups (Fig. 5, right). In contrast to 7-Nd, two of the amido ligands and the oxo are now located on the same side of the plane spanned by the Ln_3 metal centres. The coordination of the thf donor molecules is opposite to the amido ligands (Fig. 6). The Nd–O bond lengths (avg. 2.239 Å) are slightly longer than in $[Cp^*Nd(NC_5H_4NC_4H_8)]_2(\mu\text{-}O)$ (2.157(2) Å).[59] Similarly, the benzamidinato-supported complexes $[PhC(NC_6H_3iPr_2\text{-}2,6)_2]_3Ln_3(\mu_3\text{-}CH_2)(\mu_3\text{-}Me)(\mu_2\text{-}Me)_3$ (Ln = Sc, Lu) could be selectively converted into the oxo derivatives.[32]

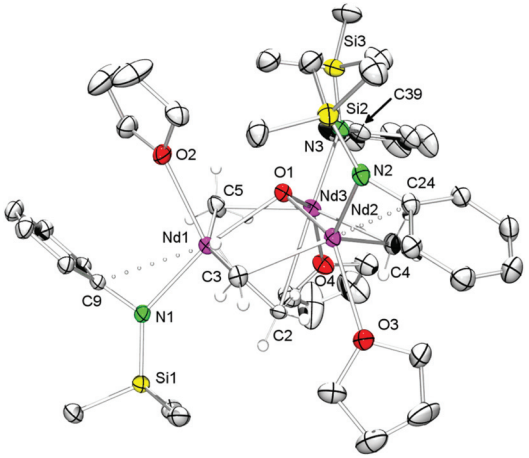

Fig. 6 Molecular structure of **8**-Nd (atomic displacement parameters are set at the 30% level). Isopropyl groups and hydrogen atoms, except for Nd–CH_3 moieties, have been omitted for clarity.

Synthesis and characterization of $[NSiMe_3(Ar)]_2Ln(AlMe_4)$ (9-Ln)

As shown in Scheme 2/route **B**, reaction of $Ln(AlMe_4)_3$ (**2**-Ln, Ln = La, Nd) with $K[NSiMe_3(Ar)]$ in *n*-hexane for 2 h and separation of precipitated $KAlMe_4$ gave $[NSiMe_3(Ar)]Ln(AlMe_4)_2$ (**5**-Ln), however, contaminated by small amounts of the bis(amide) complex $[NSiMe_3(Ar)]_2Ln(AlMe_4)$ (**9**-Ln, Ln = La, Nd), which were separated by fractional crystallization. Complexes **9**-Ln could be obtained in moderate yields *via* salt metathesis of $Ln(AlMe_4)_3$ (**2**-Ln) with two equivalents of $K[NSiMe_3(Ar)]$ in *n*-hexane at ambient temperature (Scheme 5).

The ^{1}H and $^{13}C\{^1H\}$ NMR spectra of complex **9**-La revealed one set of signals for the amido ligands and the $AlMe_4$ moiety, except for the diastereotopic aryl isopropyl groups. While the ^{1}H NMR resonances for the $NSiMe_3(Ar)$ ligand are shifted to lower fields compared to **5**-La, a high-field shift was observed for the signal of the $AlMe_4$ ligand (δ −0.47 ppm, 12H; **5**-La: δ −0.19 ppm). The resonance of the $AlMe_4$ ligand in paramagnetic **9**-Nd appeared at 10.73 ppm. Blue (**9**-Nd) and colourless (**9**-La) single crystals were obtained from saturated *n*-hexane solutions. Previously reported $Nd[NSiMe_3(Ar)]_2Cl(thf)$[60] is somewhat comparable to isomorphous **9**-Ln featuring also a four-coordinate Ln metal centre (Fig. 7). Such simple complexes $(NRR')_2Ln(alkyl)$ and $(NRR')Ln(alkyl)_2$ coordinated by non-chelating alkyl and amido ligands, however, seem to be rather scarce.[40,41,56] Complexes **9**-Ln display distorted tetrahedral coordination geometries as evidenced by large N1–Ln–C(μ_2-CH_3) angles *e.g.*, **9**-La, 122.5(2)°; **9**-Nd, 123.33(3)° (Table 3). Pronounced interactions of the Ln^{III} metal centre with the amido ligand is also evidenced by close contacts to

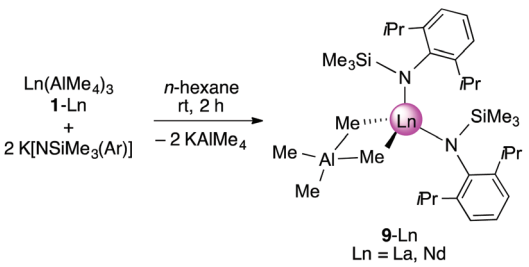

Scheme 5 Synthesis of $[NSiMe_3(Ar)]_2Ln(AlMe_4)$ (**9**-Ln, Ln = La, Nd).

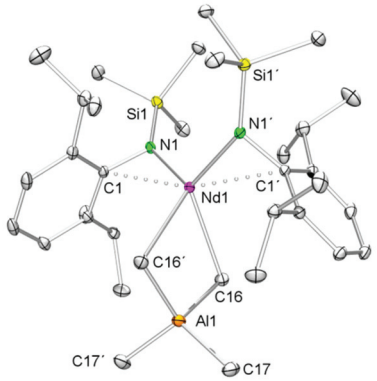

Fig. 7 Molecular structure of $[NSiMe_3(Ar)]_2Nd(AlMe_4)$ (**9**-Nd), representative of the isomorphous complexes **9**-La and **9**-Nd. Atomic displacement parameters are set at the 30% level, hydrogen atoms have been omitted for clarity.

Table 3 Selected bond lengths (Å) and angles (°) for **9**-La and **9**-Nd

	9-La	**9**-Nd
Ln1–N1	2.356(3)	2.2968(8)
Ln1–C16	2.719(4)	2.650(1)
Al1–C16	2.072(4)	2.073(1)
Al1–C17	1.979(4)	1.980(1)
Ln1···Al1	3.296(2)	3.2302(4)
Ln1···C1	2.791(3)	2.7502(9)
N1–Ln1–C16	103.73(11)	103.10(3)
Ln1–N1–C1	91.95(18)	92.29(5)

the *ipso* carbon atoms of the aryl rings (**9**-La, 2.791(7) Å; **9**-Nd, 2.7502(9) Å). The average Ln–C(μ_2-CH_3) bond lengths of 2.721 Å (**9**-La, 2.650 Å (**9**-Nd)) are shorter than in the respective metallocene complex $Cp^*_2La(AlMe_4)$ (avg. 2.849 Å), which is dimeric in the solid-state.[55]

Conclusions

The unique $[Ln_3(\mu_3\text{-}CH_2)(\mu_3\text{-}CH_3)(\mu_2\text{-}CH_3)_3]$ core structure has been achieved *via* three synthesis pathways. Such rare-earth metal methylidene complexes do form in the absence of any organoaluminium components as proven by applying alkylaluminium-free synthesis protocols. The generation of $[NSiMe_3(Ar)]_3Ln_3(\mu_3\text{-}CH_2)(\mu_3\text{-}Me)(\mu_2\text{-}Me)_3(thf)_3$ seems to be rather driven by steric constraints. A possible mechanism involves the formation of intermediate $[NSiMe_3(Ar)]LnMe_2(thf)_x$ species, which upon C–H bond activation agglomerate to the target compound. The dianionic CH_2^{2-} moiety seems to be preferentially stabilized by Ln_3 "cluster-like" entities being protected from intermolecular deactivation by a picket-fence arrangement of the amido ligands. Nevertheless the methylidene ligand retains its nucleophilic character as revealed by Tebbe-like methylenation reactions with carbonylic substrates, which concomitantly form isolable rare-earth metal oxo clusters.

Experimental section

General procedures

All operations were performed with rigorous exclusion of air and water, using standard Schlenk, high-vacuum, and glovebox techniques (MBraun MBLab; <1 ppm O_2, <1 ppm H_2O). Toluene, *n*-hexane, and tetrahydrofuran were purified by using Grubbs columns (MBraun SPS, solvent purification system) and stored in a glovebox. Benzene-d_6 and toluene-d_8 were obtained from Aldrich, degassed, dried over Na for 24 h, and filtered. Tetrahydrofuran-d_8 was obtained from Aldrich, degassed, dried over CaH_2 for four days and vacuum transferred. 9-Fluorenone was obtained from Fluka and sublimed prior to use. $[LuMe_3]_n$ (**1**-Lu),[38] homoleptic $Ln(AlMe_4)_3$ (**2**-Ln) (Ln = Y, Nd, Ho, Lu)[42,43] and $Y(GaMe_4)_3$ [53] were prepared according to literature methods. $H[NSiMe_3(Ar)]$ and $K[NSiMe_3(Ar)]$ were synthesized by a modification of the published procedure.[44,45] The NMR spectra of air and moisture sensitive compounds were recorded by using J. Young valve NMR tubes at 26 °C on a Bruker-Avance II 400 (^{1}H: 400.13 MHz; ^{13}C: 100.61 MHz) and a Bruker-Avance II 500 (^{1}H: 500.13 MHz; ^{13}C: 125.76 MHz). ^{1}H and ^{13}C shifts are referenced to internal solvent resonances and reported in parts per million relative to TMS. Coupling constants are given in Hertz. IR and DRIFT spectra were recorded on a *NICOLET 6700 FTIR* spectrometer using dried KBr and KBr windows or as Nujol mulls sandwiched between CsI plates. Elemental analyses were performed on an *Elementar Vario EL III* and an *Elementar Vario Micro Cube*.

$[NSiMe_3(Ar)]LuMe_2(thf)_2$ (4-Lu). A solution of $H[NSiMe_3(Ar)]$ (50 mg, 0.20 mmol) in *n*-hexane (1 ml) was added to a suspension of 1/*n* $[LuMe_3]_n$ (**1**-Lu) (44 mg, 0.20 mmol) in *n*-hexane (1 ml) at ambient temperature under vigorous stirring. To the orange reaction mixture thf (1 ml) was slowly added. After approximately 30 min the mixture became clear and was stirred for additional 60 min at ambient temperature. The orange solution was filtered and single crystals of **4**-Lu suitable for X-ray diffraction analysis were obtained from the thf/*n*-hexane solution at −35 °C (46 mg, 0.08 mmol, 33%). ^{1}H NMR (500 MHz, thf-d_8, 26 °C): δ = 6.97 (d, 2H, $^3J_{HH}$ = 7.6 Hz, H_{meta}, Ar), 6.77 (t, 1H, $^3J_{HH}$ = 7.6 Hz, H_{para}, Ar), 3.76 (sept, 2H, $^3J_{HH}$ = 6.9 Hz, C*H*(CH_3)$_2$), 3.58 (m, 8H, OC*H*$_2$CH$_2$), 1.73 (m, 8H, OCH$_2$C*H*$_2$), 1.18 (d, 6H, $^3J_{HH}$ = 6.9 Hz, C*H*$_3$), 1.12 (d, 6H, $^3J_{HH}$ = 6.9 Hz, C*H*$_3$), 0.05 (s, 9H, Si–C*H*$_3$), −1.06 (s, 6H, Lu–C*H*$_3$) ppm. ^{13}C{^{1}H} NMR (126 MHz, thf-d_8, −35 °C): δ = 150.8 (C_{ipso}, Ar), 145.7 (C_{ortho}, Ar), 123.8 (C_{meta}, Ar), 120.8 (C_{para}, Ar), 67.6 (thf), 29.4 (Lu–*C*H$_3$), 27.8 (*C*H(CH_3)$_2$), 26.5 (*C*H$_3$), 26.3 (*C*H$_3$), 4.4 (Si–*C*H$_3$) ppm. IR (KBr) = 3039w, 3057w, 2960s, 2888m, 2765w, 1914vw, 1856vw, 1582vw, 1462m, 1419m, 1379w, 1359w, 1342w, 1310m, 1232s, 1186m, 1141w, 1110m, 1038m, 1011m, 912s, 837vs, 738m, 621w, 570w, 527m, 445m cm^{-1}. Anal. Calcd (%) for $C_{25}H_{48}LuNO_2Si$: C 50.24, H 8.09, N 2.34. Found: C 50.11, H 8.04, N 2.35.

General procedure for the synthesis of $[NSiMe_3(Ar)]$-$Ln(AlMe_4)_2$ (5-Ln). In a glovebox, a solution of $Ln(AlMe_4)_3$ (**2**-Ln) in *n*-hexane (3 ml) was added to a vigorously stirred

suspension of K[NSiMe$_3$(Ar)] in *n*-hexane (2 ml) at ambient temperature. The reaction mixture was stirred for 2 h and the *n*-hexane solution then separated by centrifugation, decantation, and filtration. Compounds **6**-Ln were obtained by crystallization from a saturated *n*-hexane solution at −35 °C.

[NSiMe$_3$(Ar)]La(AlMe$_4$)$_2$ (5-La). Following the procedure described above, La(AlMe$_4$)$_3$ (160 mg, 0.40 mmol) and K[NSiMe$_3$(Ar)] (115 mg, 0.40 mmol) yielded **5**-La as colourless crystals. Compound **5**-La was purified and separated from co-product [NSiMe$_3$(Ar)]$_2$La(AlMe$_4$) (**9**-La) by fractional crystallization (136 mg, 0.24 mmol, 60%). ^{1}H NMR (400 MHz, C$_6$D$_6$, 26 °C): δ = 7.09–6.98 (m, 3H, H_{meta}, H_{para}, Ar), 3.12 (sept, 2H, $^3J_{HH}$ = 6.7 Hz, C*H*(CH$_3$)$_2$), 1.15 (d, 6H, $^3J_{HH}$ = 6.9 Hz, CH(C*H*$_3$)$_2$), 0.96 (d, 6H, $^3J_{HH}$ = 6.6 Hz, CH(C*H*$_3$)$_2$), 0.24 (s, 9H, Si(C*H*$_3$)$_3$), −0.19 (s, 24H, Al–C*H*$_3$) ppm. ^{13}C{^{1}H} NMR (101 MHz, C$_6$D$_6$, 26 °C): δ = 149.2 (C_{ipso}, Ar), 139.0 (C_{ortho}, Ar), 127.6 (C$_{meta}$, Ar), 127.1 (C_{para}, Ar), 28.8 (*C*H(CH$_3$)$_2$), 26.7 (*C*H$_3$), 23.9 (*C*H$_3$), 4.6 (Al–*C*H$_3$), 4.1 (Si–*C*H$_3$) ppm. IR (nujol) = 1248m, 1192m, 1110vw, 1042vw, 906m, 833m, 775m, 580w cm^{-1}. Anal. Calcd (%) for C$_{23}$H$_{50}$Al$_2$LaNSi: C 49.19, H 8.97, N 2.49. Found: C 49.59, H 8.57, N 2.45.

[NSiMe$_3$(Ar)]Nd(AlMe$_4$)$_2$ (5-Nd). Following the procedure described above, Nd(AlMe$_4$)$_3$ (81 mg, 0.21 mmol) and K[NSiMe$_3$(Ar)] (60 mg, 0.21 mmol) yielded **5**-Nd as blue crystals. Compound **5**-Nd was purified and separated from co-product [NSiMe$_3$(Ar)]$_2$Nd(AlMe$_4$) (**9**-Nd) by fractional crystallization (82.2 mg, 0.14 mmol, 67%). ^{1}H NMR (400 MHz, C$_6$D$_6$, 26 °C): δ = 11.27, 1.37, 1.24, 0.89, 0.15, 0.12, −0.43 ppm. ^{13}C{^{1}H} NMR (101 MHz, C$_6$D$_6$, 26 °C): δ = 220.8, 204.5, 152.8, 76.6, 60.3, 44.3, 5.7, 2.0 ppm. IR (KBr) = 3054s, 2964m, 2923m, 1456m, 1415m, 1361s, 1310s, 1263s, 1247m, 1228m, 1190s, 1110s, 1043s, 910s, 878m, 836s, 778m, 747m, 694s, 654m, 575m, 504m, 458s, 433s cm^{-1}. Anal. Calcd (%) for C$_{23}$H$_{50}$NAl$_2$SiNd: C 48.73, H 8.89, N 2.47. Found: C 48.53, H 8.72, N 2.44.

[NSiMe$_3$(Ar)]Ho(AlMe$_4$)$_2$ (5-Ho). Following the procedure described above, Ho(AlMe$_4$)$_3$ (75 mg, 0.18 mmol) and K[NSiMe$_3$(Ar)] (52 mg, 0.18 mmol) yielded **5**-Ho (75 mg, 0.13 mmol, 72%) as pink single crystals suitable for X-ray diffraction analysis. IR (nujol) = 1377s, 1309m, 1248m, 1227m, 1185m, 1107w, 1042w, 967w, 908m, 875m, 838m, 782m, 571m cm^{-1}. Anal. Calcd (%) for C$_{23}$H$_{50}$HoAl$_2$NSi: C 47.01, H 8.58, N 2.38. Found: C 46.92, H 9.03, N 2.34.

[NSiMe$_3$(Ar)]Y(GaMe$_4$)$_2$ (6-Y). Following the procedure described for **5**-Ln, Y(GaMe$_4$)$_3$ (74 mg, 0.16 mmol) and K[NSiMe$_3$(Ar)] (45 mg, 0.16 mmol) yielded **6**-Y as colourless crystals (53 mg, 0.09 mmol, 55%). ^{1}H NMR (500 MHz, toluene-d_8, 26 °C): δ = 7.07 (m, 3H, H_{meta}, H_{para}, Ar), 3.43 (sept, 2H, $^3J_{HH}$ = 6.7 Hz, C*H*(CH$_3$)$_2$), 1.24 (d, 6H, $^3J_{HH}$ = 6.8 Hz, C*H*$_3$), 1.10 (d, 6H, $^3J_{HH}$ = 6.6 Hz, C*H*$_3$), 0.31 (s, 9H, Si–C*H*$_3$), −0.03 (s, 24H, Ga–C*H*$_3$) ppm. ^{13}C from HSQC and HMBC (126 MHz, toluene-d_8, 26 °C): δ = 148.3 (C_{ipso}, Ar), 138.4 (C_{ortho}, Ar), 125.5 (C_{meta}, C_{para}, Ar), 27.8 (*C*H(CH$_3$)$_2$), 26.2 (*C*H$_3$), 23.0 (*C*H$_3$), 3.3 (Si–*C*H$_3$), 2.4 (Ga–*C*H$_3$) ppm. ^{89}Y NMR (500 MHz, toluene-d_8, 26 °C): δ = 477.2 ppm. IR (nujol): 1309w, 1250m, 1203w, 1105w, 1051w, 908w, 836w, 583w, 526w cm^{-1}. Anal. Calcd (%) for C$_{23}$H$_{50}$Ga$_2$NSiY: C 46.27, H 8.44 N 2.35. Found: C 46.55, H 8.45, N 2.37.

[NSiMe$_3$(Ar)]$_3$Y$_3$(μ_3-CH$_2$)(μ_2-Me)$_3$(μ_3-Me)(thf)$_3$ (7-Y). To a solution of [NSiMe$_3$(Ar)]Y(GaMe$_4$)$_2$ (**6**-Y) (76 mg, 0.13 mmol) in *n*-hexane (2 ml) two drops of thf were added. The reaction mixture was shaken and left standing for 30 min at ambient temperature. **7**-Y precipitated at −35 °C, the supernatant was decanted and the white solid dried under reduced pressure (76 mg, 0.12 mmol, 93%). Single crystals suitable for X-ray structure analysis were grown from a saturated *n*-hexane solution. The spectroscopic data were consistent with those previously published.[31]

[NSiMe$_3$(Ar)]$_3$Nd$_3$(μ_3-CH$_2$)(μ_2-Me)$_3$(μ_3-Me)(thf)$_3$ (7-Nd). To a solution of [NSiMe$_3$(Ar)]Nd(AlMe$_4$)$_2$ (**5**-Nd) (60.7 mg, 0.1 mmol) in *n*-hexane (2 ml) ten drops of thf were added. The reaction mixture was shaken and left standing for 10 min at ambient temperature. The product could be crystallized from a thf/*n*-hexane mixture at −35 °C to yield blue crystals (45.5 mg, 0.03 mmol, 90% cryst. yield). IR (KBr): 3041s, 2957s, 2868m, 1583s, 1458m, 1416s, 1380s, 1359s, 1313m, 1239s, 1193m, 1159s, 1142s, 1107s, 1041s, 1022s, 915s, 877m, 835s, 774s, 744s, 731s, 658m, 588s, 487m, 434m cm^{-1}. ^{1}H NMR (400 MHz, C$_6$D$_6$, 26 °C): δ = 13.05, 12.35, 7.98, 6.28, 3.19, 2.34, 2.10, 1.23, 0.88, −1.25 ppm. Anal. Calcd (%) for C$_{62}$H$_{116}$N$_3$O$_3$Si$_3$Nd$_3$: C, 50.71; H, 7.96; N, 2.86. Found: C, 51.28; H, 8.29; N, 2.73.

[NSiMe$_3$(Ar)]$_3$Ho$_3$(μ_3-CH$_2$)(μ_2-Me)$_3$(μ_3-Me)(thf)$_3$ (7-Ho). To a solution of [NSiMe$_3$(Ar)]Ho(AlMe$_4$)$_2$ (**5**-Ho) (66 mg, 0.11 mmol) in *n*-hexane (2 ml) excess thf was added. A pink precipitate formed. The mixture became clear after further addition of thf. The reaction mixture was shaken and left standing at −35 °C. Single crystals suitable for X-ray diffraction analysis were grown from the *n*-hexane/thf solution at −35 °C (cryst. yield: 42.9 mg, 0.03 mmol, 82%). IR (KBr): 3042w, 2959s, 2868m, 1584w, 1459m, 1418s, 1379w, 1359w, 1310m, 1240s, 1183s, 1105m, 1039w, 1014m, 903s, 837vs, 777s, 745m 666m, 521m, 435m cm^{-1}. δ_H (500 MHz, benzene-d_6) 12.41, 11.80, 9.50, 8.93, 8.66, 8.44, 7.89, 7.76, 7.71, 4.87, 2.60, 2.11, 1.59, 0.12, −0.42, −0.99, −1.46, −2.78, −4.25, −4.63 ppm. Anal. Calcd (%) for C$_{62}$H$_{116}$Ho$_3$N$_3$O$_3$Si$_3$: C, 48.65; H, 7.64; N, 2.75 Found: C 48.57, H 7.65, N 2.47.

[NSiMe$_3$(Ar)]$_3$Lu$_3$(μ_3-CH$_2$)(μ_2-Me)$_3$(μ_3-Me)(thf)$_3$ (7-Lu). A J. Young valve NMR tube was charged with **4**-Lu (12.0 mg, 0.02 mmol) and dissolved in *n*-hexane (1 ml) and dried under reduced pressure. The procedure was repeated several times. The residue was dissolved in C$_6$D$_6$. ^{1}H NMR measurements were started after approximately 10 minutes, showing that **4**-Lu had converted into **7**-Lu.[31]

[NSiMe$_3$(Ar)]$_3$Nd$_3$(μ_3-O)(μ_2-Me)$_4$(thf)$_3$ (8-Nd). To a solution of **7**-Nd (70 mg, 0.05 mmol) in *n*-hexane/thf (3 ml) a solution of 9-fluorenone in *n*-hexane/thf (3 ml) was added, shaken and left standing for 5 minutes. The blue solution turned green. Single crystals suitable for X-ray diffraction analysis were grown from the *n*-hexane/thf solution at −35 °C. Alternatively, all volatiles were removed *in vacuo* to yield **8**-Nd as a green powder, which was washed with *n*-hexane (2 × 1 ml) and dried *in vacuo* (30 mg, 0.02 mmol, 41%; 29% cryst. yield). ^{1}H NMR

(400 MHz, C_6D_6): δ = 12.17, 10.28, 8.66, 8.57, 0.50, 0.27, 0.14, −0.19, −0.41, −0.54, −3.76, −4.26 ppm. IR (KBr): 2957s, 2868m, 1457w, 1417s, 1379w, 1359w, 1311m, 1251m, 1237vs, 1192m, 1107w, 1025w, 921s, 878m, 835vs, 774m, 746w, 660w cm^{-1}. Anal. Calcd (%) for $C_{61}H_{114}N_3Nd_3O_4Si_3$: C 49.82, H 7.81, N 2.86. Found: C 50.12, H 8.04, N 2.60.

[NSiMe$_3$(Ar)]$_2$La(AlMe$_4$) (9-La). Following the procedure described for **5**-Ln, La(AlMe$_4$)$_3$ (80 mg, 0.20 mmol) and K[NSiMe$_3$(Ar)] (115 mg, 0.40 mmol) yielded **9**-La as colourless crystals (64 mg, 0.09 mmol, 44%). ^{1}H NMR (400 MHz, C_6D_6, 26 °C): δ = 7.12 (d, $^3J_{HH}$ = 7.7 Hz, 4H, H_{meta}, Ar), 7.02 (t, $^3J_{HH}$ = 7.9 Hz, 2H, H_{para}, Ar), 3.35 (sept, 4H, $^3J_{HH}$ = 6.8 Hz, CH(CH$_3$)$_2$), 1.31 (d, 12H, $^3J_{HH}$ = 7.1 Hz, CH(CH_3)$_2$), 1.09 (d, 12H, $^3J_{HH}$ = 6.5 Hz, CH(CH_3)$_2$), 0.24 (s, 18H, Si(CH_3)$_3$), −0.47 (s, 12H, Al–CH_3) ppm. ^{13}C{^{1}H} NMR (101 MHz, C_6D_6, 26 °C): δ = 146.4 (C_{ipso}, Ar), 143.3 (C_{ortho}, Ar), 127.7 (C_{meta}, Ar), 125.8 (C_{para}, Ar), 28.5 (CH(CH$_3$)$_2$), 26.8 (CH$_3$), 24.8 (CH$_3$), 4.6 (Si–CH$_3$), 4.2 (Al–CH$_3$) ppm. IR (nujol) = 1941vw, 1878vw, 1585vw, 1325s, 1306s, 1243s, 1187s, 1098w, 1037w, 911m, 833m, 777w, 577w cm^{-1}. Anal. Calcd (%) for $C_{34}H_{64}AlLaN_2Si_2$: C 56.49, H 8.92, N 3.87. Found: C 56.35, H 9.94, N 3.88.

[NSiMe$_3$(Ar)]$_2$Nd(AlMe$_4$) (9-Nd). Following the procedure described for **5**-Ln, Nd(AlMe$_4$)$_3$ (100 mg, 0.25 mmol) and K[NSiMe$_3$(Ar)] (144 mg, 0.50 mmol) yielded **9**-Nd as blue crystals (49 mg, 0.07 mmol, 27%). ^{1}H NMR (400 MHz, C_6D_6, 26 °C): δ = 10.73, 6.39, 3.13, 1.37, 1.23, 1.21, 1.19, 0.88, 0.87, 0.63, 0.15, 0.11 ppm. ^{13}C{^{1}H} NMR (101 MHz, C_6D_6, 26 °C): δ = 197.0, 149.5, 108.4, 36.1, 27.8, 23.0, 3.2, 1.2, −3.1 ppm. IR (KBr) = 1684w, 1304m, 1250m, 1187w, 1042w, 908m, 838m, 721m cm^{-1}. Anal. Calcd (%) for $C_{34}H_{64}AlN_2NdSi_2$: C 56.07, H 8.86, N 3.85. Found: C 56.01, H 9.80, N 3.80.

Reactivity of 7-Nd toward 9-fluorenone. In a glovebox, compound 7-Nd dissolved in benzene-d_6 was placed in a *J. Young* valve NMR tube and 1 equiv. of 9-fluorenone was added. The NMR tube was shaken several times and the ^{1}H NMR spectra were recorded after 10 min. The reaction mixture turned slightly brown upon addition of 9-fluorenone and decolourized immediately. The substrate was converted quantitatively. For the addition of 2–5 equivalents of the carbonylic reagent, the *J. Young* valve NMR tube was transferred into the glovebox and the same procedure as described for the first equivalent was followed. After addition of the third equivalent substrate the mixture kept the brown colour. ^{1}H NMR (500 MHz, C_6D_6, 26 °C) after addition of 1 equiv. 9-fluorenone: δ = 9.84, 9.66, 9.26, 8.63, 7.50 (d, 2H, $^3J_{HH}$ = 7.4 Hz, Ar), 7.47 (d, 2H, $^3J_{HH}$ = 7.4 Hz, Ar), 7.09 (t, 4H, $^3J_{HH}$ = 7.4 Hz, Ar), 6.43, 6.26, 6.10, 5.79 (s, 2H, CH_2), 4.86, 3.72, 0.12, −0.56, −2.46, −3.99 ppm.

X-ray crystallography and crystal structure determination of 4-Lu, 5-Ln, 6-Y, 7-Ln, 8-Nd, and 9-Ln

Crystals of **5**-Ln, **6**-Y and **9**-Ln were grown by standard techniques from saturated solutions using *n*-hexane or *n*-hexane/thf (**4**-Lu, **7**-Ln and **8**-Nd) at −40 °C. Suitable single crystals for X-ray structure analyses were selected in a glovebox and coated with Parabar 10312 and fixed on a nylon loop/glass fiber. Data for **4**-Lu, **5**-La, **5**-Nd, **5**-Ho, **6**-Y, **7**-Nd, **7**-Ho and **8**-Nd were collected on a Stoe IPDS 2T instrument equipped with a fine focus sealed tube and graphite monochromator using MoKα radiation (λ = 0.71073 Å) performing ω scans. Raw data were collected and integrated using Stoe's X-Area software package.[61] A numerical absorption correction based on crystal shape optimization was applied using Stoe's X-Red[62] and X-Shape.[63] X-ray data for **9**-Ln were collected on a Bruker AXS, TXS rotating anode instrument using a Pt^{135} CCD detector, and graphite monochromator using MoK$_\alpha$ radiation (λ = 0.71073 Å). The Data collection strategy was determined using COSMO[64] employing ω- and ϕ scans. Raw data were processed using APEX[64] and SAINT,[64] corrections for absorption effects were applied using SADABS.[64] The structure was solved by direct methods and refined against all data by full-matrix least-squares methods on F^2 using SHELXTL[64] and ShelXle.[65] All Graphics were produced employing ORTEP-3[66] and POV-Ray.[67] Further details of the refinement and crystallographic data are listed in Table S1† and in the CIF files. CCDCs 1410385–1410394 contain all the supplementary crystallographic data for this paper.

Acknowledgements

We are grateful to the German Science Foundation for support (Grant: AN 238/15-1).

References

1 T. M. Trnka and R. H. Grubbs, *Acc. Chem. Res.*, 2001, **34**, 18.
2 R. H. Grubbs, *Angew. Chem., Int. Ed.*, 2006, **45**, 3760.
3 P. de Frémont, N. Marion and S. P. Nolan, *Coord. Chem. Rev.*, 2009, **253**, 862.
4 Z.-L. Xue and L. A. Morton, *J. Organomet. Chem.*, 2011, **696**, 3924.
5 D. J. Mindiola and J. Scott, *Nat. Chem.*, 2011, **3**, 15.
6 O. T. Summerscales and J. C. Gordon, *RSC Adv.*, 2013, **3**, 6682.
7 J. Kratsch and P. W. Roesky, *Angew. Chem., Int. Ed.*, 2014, **53**, 376.
8 J. W. Herndon, *Coord. Chem. Rev.*, 2015, **286**, 30.
9 R. R. Schrock, *J. Am. Chem. Soc.*, 1974, **96**, 6796.
10 R. R. Schrock, *Angew. Chem., Int. Ed.*, 2006, **45**, 3748.
11 L. J. Guggenberger and R. R. Schrock, *J. Am. Chem. Soc.*, 1975, **97**, 6578.
12 R. R. Schrock, *J. Am. Chem. Soc.*, 1975, **97**, 6577.
13 M. Kamitani, B. Pinter, C.-H. Chen, M. Pink and D. J. Mindiola, *Angew. Chem., Int. Ed.*, 2014, **53**, 10913.
14 K. Searles, K. Keijzer, C.-H. Chen, M.-H. Baik and D. J. Mindiola, *Chem. Commun.*, 2014, **50**, 6267.
15 J. E. Kickham, F. Guérin and D. W. Stephan, *J. Am. Chem. Soc.*, 2002, **124**, 11486.

16 P. Wei and D. W. Stephan, *Organometallics*, 2003, **22**, 1992.
17 G. Theurkauff, A. Bondon, V. Dorcet, J.-F. Carpentier and E. Kirillov, *Angew. Chem., Int. Ed.*, 2015, **54**, 6343.
18 R. E. von H. Spence, D. J. Parks, W. E. Piers, M.-A. MacDonald, M. J. Zaworotko and S. J. Rettig, *Angew. Chem., Int. Ed. Engl.*, 1995, **34**, 1230.
19 F. N. Tebbe, G. W. Parshall and G. S. Reddy, *J. Am. Chem. Soc.*, 1978, **100**, 3611.
20 R. Thompson, E. Nakamaru-Ogiso, C.-H. Chen, M. Pink and D. J. Mindiola, *Organometallics*, 2013, **33**, 429.
21 J. Scott, H. Fan, B. F. Wicker, A. R. Fout, M.-H. Baik and D. J. Mindiola, *J. Am. Chem. Soc.*, 2008, **130**, 14438.
22 R. Litlabø, M. Zimmermann, K. Saliu, J. Takats, K. W. Törnroos and R. Anwander, *Angew. Chem., Int. Ed.*, 2008, **47**, 9560.
23 M. Zimmermann, J. Takats, G. Kiel, K. W. Törnroos and R. Anwander, *Chem. Commun.*, 2008, 612.
24 L. C. H. Gerber, E. Le Roux, K. W. Törnroos and R. Anwander, *Chem. – Eur. J.*, 2008, **14**, 9555.
25 W. Huang, C. T. Carver and P. L. Diaconescu, *Inorg. Chem.*, 2011, **50**, 978.
26 A. Venugopal, I. Kamps, D. Bojer, R. J. F. Berger, A. Mix, A. Willner, B. Neumann, H.-G. Stammler and N. W. Mitzel, *Dalton Trans.*, 2009, 5755.
27 D. Bojer, B. Neumann, H.-G. Stammler and N. W. Mitzel, *Chem. – Eur. J.*, 2011, **17**, 6239.
28 D. Bojer, B. Neumann, H.-G. Stammler and N. W. Mitzel, *Eur. J. Inorg. Chem.*, 2011, **2011**, 3791.
29 D. Bojer, A. Venugopal, A. Mix, B. Neumann, H.-G. Stammler and N. W. Mitzel, *Chem. – Eur. J.*, 2011, **17**, 6248.
30 H. M. Dietrich, K. W. Törnroos and R. Anwander, *J. Am. Chem. Soc.*, 2006, **128**, 9298.
31 M. Zimmermann, D. Rauschmaier, K. Eichele, K. W. Törnroos and R. Anwander, *Chem. Commun.*, 2010, **46**, 5346.
32 J. Hong, L. Zhang, X. Yu, M. Li, Z. Zhang, P. Zheng, M. Nishiura, Z. Hou and X. Zhou, *Chem. – Eur. J.*, 2011, **17**, 2130.
33 G. Luo, Y. Luo, J. Qu and Z. Hou, *Organometallics*, 2015, **34**, 366.
34 W.-X. Zhang, Z. Wang, M. Nishiura, Z. Xi and Z. Hou, *J. Am. Chem. Soc.*, 2011, **133**, 5712.
35 T. Li, M. Nishiura, J. Cheng, Y. Li and Z. Hou, *Chem. – Eur. J.*, 2012, **18**, 15079.
36 J. Hong, L. Zhang, K. Wang, Y. Zhang, L. Weng and X. Zhou, *Chem. – Eur. J.*, 2013, **19**, 7865.
37 K. Wang, G. Luo, J. Hong, X. Zhou, L. Weng, Y. Luo and L. Zhang, *Angew. Chem., Int. Ed.*, 2014, **53**, 1053.
38 H. M. Dietrich, G. Raudaschl-Sieber and R. Anwander, *Angew. Chem., Int. Ed.*, 2005, **44**, 5303.
39 M. Zimmermann, R. Litlabø, K. W. Törnroos and R. Anwander, *Organometallics*, 2009, **28**, 6646.
40 Y. Luo, Y. Yao, W. Li, J. Chen, Z. Zhang, Y. Zhang and Q. Shen, *J. Organomet. Chem.*, 2003, **679**, 125.
41 Y. Luo, M. Nishiura and Z. Hou, *J. Organomet. Chem.*, 2007, **692**, 536.
42 W. J. Evans, R. Anwander and J. W. Ziller, *Organometallics*, 1995, **14**, 1107.
43 M. Zimmermann, N. Å. Frøystein, A. Fischbach, P. Sirsch, H. M. Dietrich, K. W. Törnroos, E. Herdtweck and R. Anwander, *Chem. – Eur. J.*, 2007, **13**, 8784.
44 Y. W. Chao, P. A. Wexler and D. E. Wigley, *Inorg. Chem.*, 1989, **28**, 3860.
45 C. Schädle, C. Meermann, K. W. Törnroos and R. Anwander, *Eur. J. Inorg. Chem.*, 2010, **2010**, 2841.
46 R. Anwander, M. G. Klimpel, H. M. Dietrich, D. J. Shorokhov and W. Scherer, *Chem. Commun.*, 2003, 1008.
47 H. M. Dietrich, C. Zapilko, E. Herdtweck and R. Anwander, *Organometallics*, 2005, **24**, 5767.
48 M. Zimmermann, K. W. Törnroos, H. Sitzmann and R. Anwander, *Chem. – Eur. J.*, 2008, **14**, 7266.
49 J. Holton, M. F. Lappert, D. G. H. Ballard, R. Pearce, J. L. Atwood and W. E. Hunter, *J. Chem. Soc., Chem. Commun.*, 1976, 480.
50 H. M. Dietrich, H. Grove, K. W. Törnroos and R. Anwander, *J. Am. Chem. Soc.*, 2006, **128**, 1458.
51 R. R. Schrock and P. R. Sharp, *J. Am. Chem. Soc.*, 1978, **100**, 2389.
52 M. Zimmermann, F. Estler, E. Herdtweck, K. W. Törnroos and R. Anwander, *Organometallics*, 2007, **26**, 6029.
53 W. J. Evans, R. Anwander, R. J. Doedens and J. W. Ziller, *Angew. Chem., Int. Ed. Engl.*, 1994, **33**, 1641.
54 H. M. Dietrich, C. Meermann, K. W. Törnroos and R. Anwander, *Organometallics*, 2006, **25**, 4316.
55 H. M. Dietrich, K. W. Törnroos, E. Herdtweck and R. Anwander, *Organometallics*, 2009, **28**, 6739.
56 B. Shen, L. Ying, J. Chen and Y. Luo, *Inorg. Chim. Acta*, 2008, **361**, 1255.
57 J. P. Collman, *Acc. Chem. Res.*, 1977, **10**, 265.
58 R. C. Hartley, J. Li, C. A. Main and G. J. McKiernan, *Tetrahedron*, 2007, **63**, 4825.
59 W. J. Evans, B. L. Davis, G. W. Nyce, J. M. Perotti and J. W. Ziller, *J. Organomet. Chem.*, 2003, **677**, 89.
60 H. Schumann, J. Winterfeld, E. C. E. Rosenthal, H. Hemling and L. Esser, *Z. Anorg. Allg. Chem.*, 1995, **621**, 122.
61 *X-Area v. 1.55*, Stoe & Cie GmbH, Darmstadt, Germany, 2009.
62 *X-Red 32 v. 1.53*, Stoe & Cie GmbH, Darmstad, Germany, 2009.
63 *X-Shape v.2.12.2*, Stoe & Cie GmbH, Darmstadt, Germany, 2009.
64 G. M. Sheldrick, *Acta Crystallogr., Sect. C: Cryst. Struct. Commun.*, 2015, **71**, 3.
65 C. B. Hübschle, G. M. Sheldrick and B. Dittrich, *J. Appl. Crystallogr.*, 2011, **44**, 1281.
66 L. J. Farrugia, *J. Appl. Crystallogr.*, 1997, **30**, 565.
67 *POV-Ray v. 3.6*, Persistence of Vision Pty. Ltd., Williamstown, Victoria, Australia, 2004. http://www.povray.org/.